Actinomycin D Binds Strongly and Dissociates Slowly at the dGpdC Site with Flanking T/T Mismatches†

Chengdi Liu and Fu-Ming Chen*

Department of Chemistry, Tennessee State University, Nashville, Tennessee 37209-1561

Received May 2, 1996; Revised Manuscript Received August 12, 1996⊗

ABSTRACT: Comparative electrophoretic, thermal denaturation, and spectroscopic studies with dodecamers of the form d(ATTA-XGCX-TAAT) and their self-complementary counterparts suggest that actinomycin D (ACTD) binds strongly to a 5′GC3′ site with flanking T/T mismatches and moderately to that with C/C mismatches but weakly to those with other G/G or A/A mismatches. The relative binding order is found to be T/T > C/C > G/G > A/A. The ACTD binding affinity for the GC site with T/T mismatches is comparable to the strong binding of self-complementary -XGCY- sequences. Both the ACTD association and dissociation kinetics at the GC site with flanking T/T mismatches require two-exponential fits. The slow component of the association rates is slower than those of the self-complementary sequences, whereas that of the dissociation is only slightly faster than that of the -TGCA- sequence. Interestingly, the slow component of dissociation is decidedly slower than those of -AGCT- and -CGCG- sites and is more than an order of magnitude slower than those with C/C, G/G, and A/A mismatches. These kinetic results are further corroborated by fluorescence measurements using 7-amino-ACTD, a fluorescent analog of ACTD. In addition, fluorescence and absorbance spectral characteristics indicate that the binding mode at the GC site with flanking T/T mismatches resembles those of strong-binding self-complementary -XGCY- sites which are known to be intercalative in nature. The observed slow ACTD dissociation at the T/T-mismatched site suggests that the minor-groove environment near the T/T-mismatched pairs provides favorable interactions with the pentapeptide rings of the drug, whereas the others, especially those of bulkier purine/purine mismatches, result in less favorable interactions.

Actinomycin D (ACTD) is an antitumor antibiotic that contains a 2-aminophenoxazin-3-one chromophore and two cyclic pentapeptide lactones. Its DNA binding mode and base sequence specificity have been well characterized by X-ray crystallography (Sobell & Jain, 1972; Takusagawa et al., 1982; Kamitori & Takusagawa, 1992), footprinting (Lane et al., 1983; Scamrov & Beabealashvilli, 1983; Van Dyke & Dervan, 1983; Van Dyke et al., 1983; Fox & Waring, 1984; White & Phillips, 1989; Rehfuss et al., 1990; Goodisman et al., 1992; Goodisman & Dabrowiak, 1992), hydrodynamic (Muller & Crothers, 1968), and spectroscopic (Krugh, 1972; Patel, 1974; Krugh et al., 1977; Brown et al., 1984; Scott et al., 1988a,b; Zhou et al., 1989; Brown et al., 1994) measurements. The most recent crystallographic study with $d(GAAGCTTC)_2$ has largely confirmed the earlier proposed intercalative model and provided additional structural details (Kamitori & Takusagawa, 1994). The complex is formed by the phenoxazinone chromophore intercalating into the 5′GC3′ sequence from the minor groove, with the two cyclic pentapeptide rings resting on both sides of the minor groove and covering four base pairs of DNA. Four threonine−guanine hydrogen bonds and two additional hydrogen bonds between the N2 amino group of phenoxazone and the DNA backbone are formed. The preference of this drug for the 5′GpC3′ step is, thus, the consequence of these threonine−guanine hydrogen-bond formations. These essential drug−DNA hydrogen bonds are protected by the cyclic pentapeptides, which effectively shield them from solvent exposure. The size of the four-base-paired binding site suggests that the binding characteristics of ACTD to the GC site may be affected by the adjacent flanking base pairs. Indeed, studies with self-complementary as well as non-self-complementary -XGCY-containing decamers (Chen, 1988, 1992) have revealed that the binding affinity and dissociation kinetics of this drug are greatly affected by the nature of X and Y bases. For example, ACTD binds strongly to and dissociates very slowly from the -TGCA- site, whereas it binds weakly and dissociates very rapidly from the -GGCC- sequence. Similar adjacent base-pair effects had also been observed by others (Aivasashvilli & Beabealashvilli, 1983; Rill et al., 1989). In addition to the observed GC sequence preference, there have been other reports to indicate that this drug can also bind to some non-GpC sites (Snyder et al., 1989; Waterloh & Fox, 1992; Bailey & Graves, 1993). Of particular interest are the observations of ACTD binding to some single-stranded DNA (Wadkins & Jovin, 1991) and of strong ACTD binding and slow dissociation from the -TGGGT- duplex site (Rill et al., 1989; Bailey, S. A., et al., 1994).

DNA base-pair mismatches can sometimes serve as initiators or intermediates in a mutagenic pathway, and they may be introduced during replication (Modrich, 1987), recombination (Akiyama et al., 1989), or other chemical events. These sites can also serve as preferential targets for drugs or carcinogens. Thus, the effects of base-pair mismatches on DNA structures (Hunter, 1992) and their ligand interactions are of considerable interest, as they may have

† Research Supported by USPHS Grant CA-42682 and Army Medical Research Grant DAMD17-94-J-4474.

* Corresponding author.

⊗ Abstract published in *Advance ACS Abstracts,* December 1, 1996.

S0006-2960(96)01060-4 CCC: $12.00

relevance in DNA repair, transcription, replication, and activation of damaged genes. A logical extension of our earlier studies on the adjacent base-pair effects on the ACTD binding to a GC site would be to investigate the effects of the flanking base mismatches on the affinity and kinetic behaviors of this preferred GpC sequence. This report describes results of such studies but focuses only on ACTD binding and kinetic investigations on GC sites flanked by homobase mismatches. Comparative studies using dodecamers containing self-complementary -XGCY- and non-self-complementary -XGCX- sequences were carried out to accomplish our objectives.

MATERIALS AND METHODS

Synthetic oligonucleotides were purchased from Research Genetics, Huntsville, AL, and used without further purification. These oligomers were purified by the vendor via reverse-phase oligonucleotide purification cartridges and exhibited single-band electrophoretic mobilities in denaturating PAGE with stated purities of ≥95%. All experiments were carried out in 10 mM HEPPS [*N*-(2-hydroxyethyl)-piperazine-*N*′-propanesulfonic acid] buffer solutions of pH 8 containing 0.1 M NaCl and 1 mM $MgCl_2$. Concentrations of these oligomers (per nucleotide) were determined by measuring the absorbances at 260 nm after melting, with use of extinction coefficients obtained via nearest-neighbor approximation using mono- and dinucleotide values tabulated in Fasman (1975). The extinction coefficients used for drug concentration determination are 24 500 M^{-1} cm^{-1} at 440 nm for ACTD and 23 600 M^{-1} cm^{-1} at 528 nm for 7-amino-ACTD. Absorption spectra were measured with a Cary 1E spectrophotometric system. Thermal denaturation experiments were carried out with 1-cm semimicro cells by monitoring absorbances at 275 nm. A heating rate of 0.5 °C/min was maintained by the temperature controller accessory. Spectral titrations were carried out at 20 °C and absorbance changes at 427 and 480 nm were used to obtain Scatchard plots. Fluorescence measurements were made with an SLM 48000S system. Fluorescence kinetic measurements were made by monitoring either 650 or 600 nm for the association and 600 nm for the 1% SDS- (sodium dodecyl sulfate-) induced dissociation with 560-nm excitation and using a stirrer accessory. Absorbance kinetic measurements were made by using a stirrer accessory with 427- and 453-nm monitorings for the ACTD association and SDS-induced dissociation, respectively. Kinetic rate parameters were extracted using a nonlinear least-squares fit program of Micromath (Salt Lake City, Utah).

CD (circular dichroic) spectra were measured with a Jasco J-500A recording spectropolarimeter using water-jacketed cylindrical cells of 1-cm path length. CD kinetic measurements were made by monitoring ellipticity changes at 293 nm for both association and dissociation. Electrophoretic measurements were made on a Pharmacia Phast System using 20% polyacrylamide native gels at 200 V with appropriate pre- and postloading run times at different temperatures. PhastGel buffer strips containing 0.25 M Tris, pH 8.8, were used and the gels were developed by silver staining.

RESULTS

Rationale for the Choice of Oligomers. Dodecamers of the form d(ATTA-XGCX-TAAT), where X = A, T, G, or C, were chosen for this study. Except for the X base, this sequence is self-complementary and contains a single GC site at the center. Thus, several conformations can be envisioned to exist in solutions: a single-stranded form (Ia); a monomeric hairpin consisting of a 4-base-paired stem and a 4-base loop (I); a dimeric form with duplex side arms and a central 5′GC3′ duplex step flanked by X/X mismatches (II); a dimeric form with duplex side arms and a 4-base bulge in the central region (IIa); a dimeric form with a central GC duplex step attached to four single-stranded side arms (IIb); and higher multimeric species such as a cruciformlike tetramer having two ATTA/TAAT and two ATTAXGCX/XGCXTAAT duplex arms. The hairpin form I should predominate in the monomeric conformations, whereas duplex form II is expected to be more stable than forms IIa and IIb in the dimeric species. Furthermore, the presence of base mismatches will significantly destabilize the dimeric duplex conformations and thus favor hairpin formation near room temperatures. The hairpin form would, however, place the GC sequence at the loop region with only A·T base pairings in the duplex stem. Its ACTD binding affinity would, consequently, be expected to greatly diminish. Despite the anticipated multiconformational states and the dominant presence of hairpin conformations in solutions, it follows that if ACTD binds strongly to a duplex GC sequence with flanking base mismatches, it may further shift the equilibrium to favor the dimeric duplex for additional binding and further conformational shifts to result in a predominance of drug complexation with dimeric duplexes. Comparative studies of these oligomers will, consequently, yield the relative binding order of these mismatched sequences, and parallel studies with the corresponding self-complementary dodecamers containing the -XGCY- sequences will provide comparison with the known strong binding sites. The additional rationale for studying the self-complementary dodecamers is to provide further evidence on the effect of adjacent base pairs on the ACTD binding characteristics at the GC site, as revealed by our earlier studies with decamers of the form d(ATA-XGCY-TAT) (Chen, 1988, 1992).

Absorbance Spectral Evidence of Strong ACTD Binding for GpC with T/T Mismatches. DNA binding to ACTD results in the depression and enhancement of absorbance intensities at the 427- and 480-nm regions, respectively. Thus, a qualitative ranking of relative ACTD binding affinities of different sequences can be achieved by simply comparing the absorbance intensity alterations near these regions at the same [nucleotide]/[drug] (P/D) ratio. The absorption difference spectra of 5 μM ACTD in the presence (P/D = 20) and in the absence of DNA are compared in Figure 1 for the self-complementary (panel A) and mismatched (panel B) dodecamers. Consistent with our earlier findings with decamers (Chen, 1988), ACTD's affinity for the -GGCC- site is considerably weaker than for the other three self-complementary -XGCY- sequences, which exhibit very similar intensity alterations (panel A). Interestingly, the absorbance changes induced by ACTD binding to the dodecamer containing T/T mismatches are sizable and are in fact comparable to the self-complementary counterparts in terms of magnitude as well as spectral characteristics. Comparison among the mismatched dodecamers (Figure 1B) further suggests a qualitative ranking of binding order to be T/T > C/C > G/G > A/A for the flanking mismatched pairs.

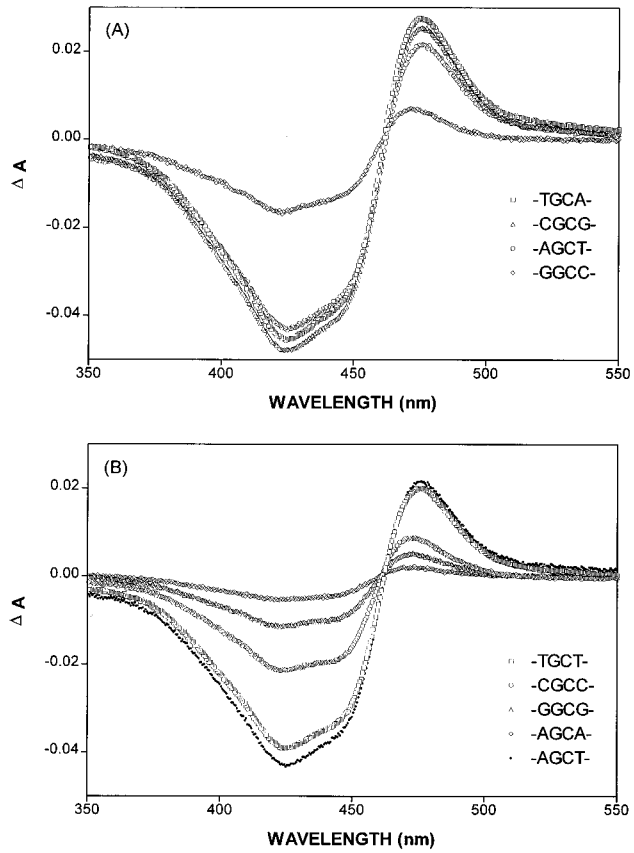

FIGURE 1: Comparison of absorption difference spectra (ACTD/DNA − ACTD) at 20 °C for solutions containing 5 μM ACTD in the absence (P/D = 0) and in the presence (P/D = 20) of self-complementary dodecamers of the form d(ATTA-XGCY-TAAT) (panel A) and mismatched dodecamers of the form d(ATTA-XGCX-TAAT) (panel B, with -AGCT- added for comparison). Spectral measurements were made in HEPPS buffer, pH 8/0.1 M NaCl, using cuvettes of 1-cm path length.

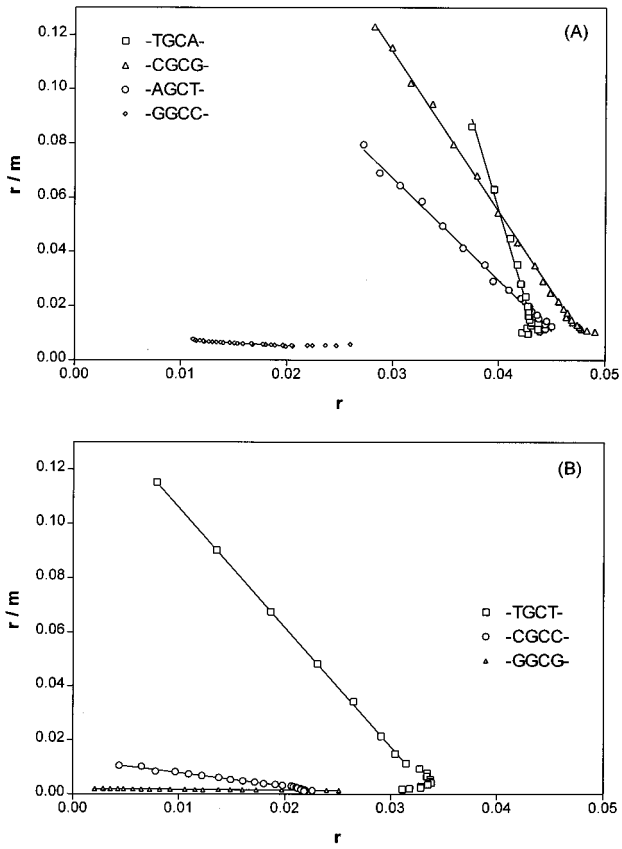

FIGURE 2: Comparison of Scatchard plots for self-complementary (panel A) and mismatched (panel B) dodecamers at 20 °C. Absorbance differences between 427 and 480 nm were employed to construct the binding isotherms. Solid lines are those of linear least-squares fits on the linear portions of the data points using the simple Scatchard equation $r / m = K_a (n - r)$, where r is the ratio of bound drug to DNA base concentrations, n is the saturation binding density, K_a is the apparent association constant, and m is the free drug concentration. Titrations in panel A were carried out by adding aliquots of DNA stock to an ACTD solution to result in nearly constant ACTD concentrations (4−5 μM) and P/D values ranging from 1 to 55 or less. Titrations in panel B were made via adding aliquots of ACTD stock to a DNA solution to result in nearly constant nucleotide concentrations (95−100 μM) and P/D values ranging from 5 to 230. Experiments were carried out in pH 8 buffer solutions containing 0.1 M NaCl and using a stirrer accessory with 1-cm cells.

Scatchard Plots. To obtain more quantitative binding parameters, absorbance spectral titrations were carried out in which aliquots of DNA stock were progressively added to an ACTD solution. The titration data at fixed wavelengths were converted to Scatchard plots (Figure 2A) for the self-complementary dodecamers. It is apparent that the plots are approximately linear, with -GGCC- exhibiting much weaker binding (~0.2 μM^{-1}) than the other three sequences (4−13 μM^{-1}) (see Table 1). In contrast, the plots for the mismatched dodecamers (not shown) exhibit unusual curvatures as if the initial low P/D data points were emanating from the origin and subsequently revert to "normal" linear plots at higher P/D. These curvatures are likely the consequence of the chosen mode of titration in which the initial additions of DNA result in much lower DNA concentrations that are less conducive to duplex formation for these mismatched oligomers even in the presence of ACTD. This situation continues with each titration point until a critical DNA concentration is reached where the duplex formation is now more favorable and the Scatchard plot appears to behave in a normal manner.

To circumvent such effects, an alternative mode of titration was employed in which aliquots of ACTD solution were progressively added to a concentrated DNA solution to result in nearly constant DNA concentrations during the course of spectral titration. The Scatchard plots for the mismatched dodecamers with use of this method are shown in Figure 2B and the binding parameters extracted via linear least-squares fits are summarized in Table 1. It is apparent that

Table 1: Comparison of Melting and ACTD Binding Parameters for Dodecamers[a]

oligomer	K (μM^{-1})	n/duplex	t_m^o (°C)	t_m (°C)
d(ATTA-TGCA-TAAT)	13.1	1.1	34.0	46.8
d(ATTA-AGCT-TAAT)	3.8	1.1	35.5	41.5
d(ATTA-CGCG-TAAT)	5.9	1.2	42.5	53.0
d(ATTA-GGCC-TAAT)	~0.2		39.4	44.8
d(ATTA-AGCA-TAAT)	0.05 (0.037)		<10	
d(ATTA-TGCT-TAAT)	4.4 (5.1)	0.8	<10	31.0
d(ATTA-GGCG-TAAT)	0.024 (0.094)		<10	<20
d(ATTA-CGCC-TAAT)	0.49 (0.29)	0.6	<10	23.3

[a] t_m^o is the estimated dimeric duplex melting temperature of 40 μM DNA (nucleotide) via 275-nm monitoring in pH 8 buffer containing 0.1 M NaCl. t_m is the melting temperature of 40 μM DNA (nucleotide) in the presence of 5 μM ACTD. Values in parentheses are those obtained via model fitting (eqs 1−3) to the experimental binding isotherms in which titrations were carried out by progressively adding aliquots of DNA stock into an ACTD solution.

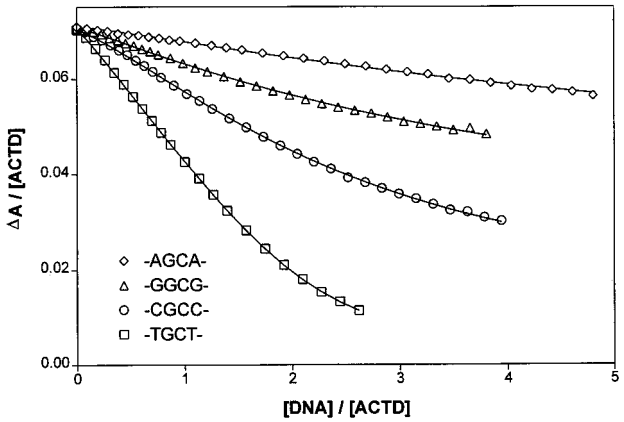

FIGURE 3: Comparison of experimental equilibrium binding isotherms with the fitted curves (solid curves) using the model presented in the text for the mismatched dodecamers of the form d(ATTA-XGCX-TAAT) at 20 °C. Experimental conditions and the titration procedures are similar to those of Figure 2A in which aliquots of DNA stock were progressively added to a 5 μM ACTD solution. ΔA corresponds to the absorbance difference of 427 and 480 nm, whereas [ACTD] is expressed in micromolar.

the ACTD binding affinity of the T/T-mismatched oligomer of 4.4 μM^{-1}, as revealed by the slope, is comparable to the strong-binding self-complementary sequences and is seen to be somewhat weaker than -TGCA- but slightly stronger than -AGCT-. In contrast to the extracted binding densities of around 0.046 (or 1.1 drug molecule/duplex) for the self-complementary sequences, the T/T-mismatched dodecamer extrapolated to approximately 0.034 (or 0.8 drug molecule/duplex). The lower binding densities of less than 1 drug molecule/duplex as exhibited by the mismatched oligomers are consistent with the significant presence of weak or non-binding hairpin and other conformations in these mismatched oligomers.

Fitting the Binding Isotherms with a Binding Model. To investigate the possibility of extracting binding constants for those isotherms which exhibit unusually curved Scatchard plots in the nearly constant [ACTD] mode of titration, the following simple model was assumed: the monomeric hairpin (L) is in dynamic equilibrium with the dimeric duplex (L_2), but only the dimeric duplex binds with the drug (S) to form a 1:1 drug to DNA complex (L_2S):

$$2\,L \overset{K_L}{\Longleftrightarrow} L_2 \qquad \text{and} \qquad L_2 + S \overset{K_1}{\Longleftrightarrow} L_2S$$

By means of equations for the mass balances of DNA (in strand) and ACTD, the following equations can be derived:

$$2(S_t - S)(1 + K_1S) + [K_1S\,(S_t - S)/K_L]^{1/2} - L_tK_1S = 0 \quad (1)$$

$$L_2 = (S_t - S)/K_1S \quad (2)$$

$$A = \epsilon_S S + \epsilon_1 S K_1 L_2 \quad (3)$$

where ϵ_S and ϵ_1 are the extinction coefficients of the free and bound drugs and S_t and L_t are the total drug and DNA strand concentrations, respectively. For simplicity, brackets were not used to represent concentrations. Nonlinear least-squares fits of the experimental binding isotherms with these equations are excellent and can be seen in Figure 3. The apparent good fit at the low P/D region where the Scatchard plots exhibit unusual curvature is particularly gratifying. The extracted binding constants are also included in Table 1 for comparison. The plausibility of the assumed model and the validity of the titration data are further strengthened by the extracted binding constants being in reasonable agreement with those obtained via Scatchard plots employing an alternative mode of titration as well as the binding orders established via the absorbance difference spectra.

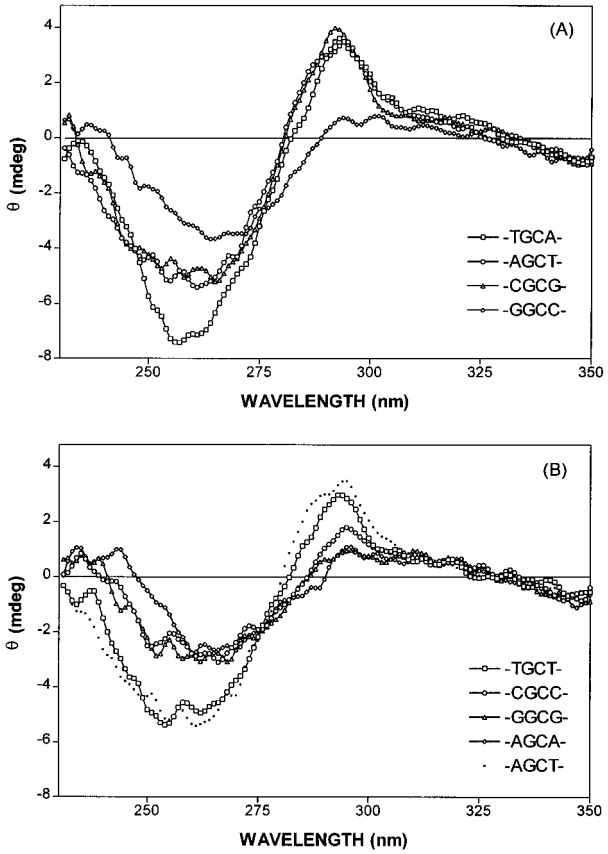

FIGURE 4: Comparison of CD difference spectra (ACTD/DNA - DNA) of 5 μM ACTD in 40 μM of self-complementary dodecamers of the form d(ATTA-XGCY-TAAT) (panel A) and mismatched dodecamers of the form d(ATTA-XGCX-TAAT) (panel B, with -AGCT- added for comparison). Measurements were made with 1-cm water-jacketed cylindrical cells at room temperatures.

CD Spectral Evidence of ACTD Binding. The effect of ACTD binding to a DNA duplex on the CD spectral characteristics is to induce sizable positive and negative CD intensities at the 293- and 255-nm regions, respectively. Thus, qualitative ACTD binding affinities for these oligomers can also be obtained via difference CD (ACTD/DNA − DNA) spectral comparison. The CD difference spectra of the dodecamers are compared in Figure 4. Except for -GGCC-, the three self-complementary sequences induce sizable and similar CD near 293 nm (panel A). In contrast, the dodecamer with T/T mismatches exhibits a larger CD difference spectrum than those of the other mismatched oligomers (panel B, with -AGCT- added for comparison) and is comparable to those of the self-complementary counterparts. The CD results are, thus, consistent with the relative binding order established via absorbance measurements.

ACTD Dissociates Slowly from d(ATTA-TGCT-TAAT). The representative non-stopped-flow-measurable dissociation kinetic traces are shown in Figure 5 and the results of least-squares fits are summarized in Table 2. It is immediately

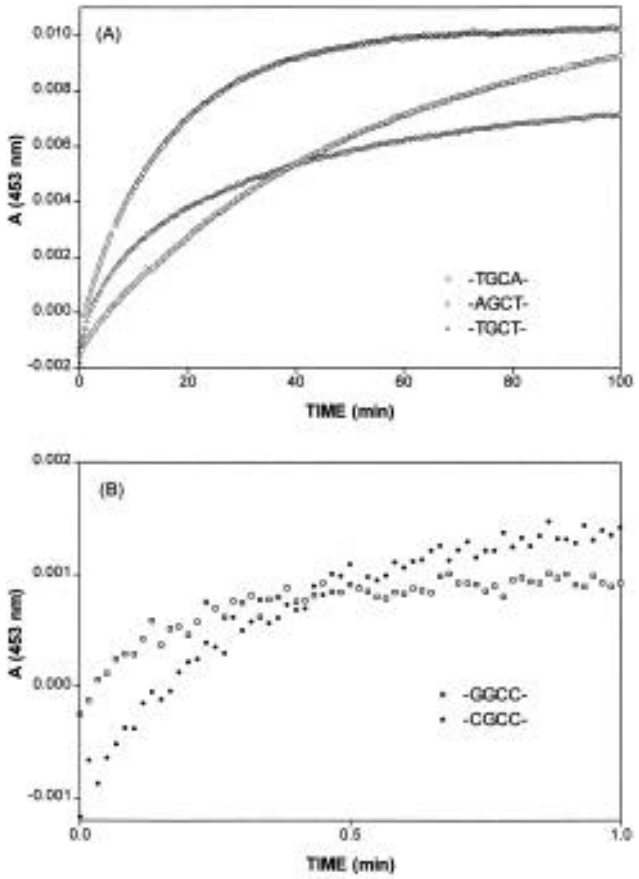

FIGURE 5: Representative 1% SDS-induced ACTD dissociation kinetic traces at 20 °C. (Panel A) Comparison of d(ATTA-TGCT-TAAT) (△) with self-complementary d(ATTA-TGCA-TAAT) (□) and d(ATTA-AGCT-TAAT) (○). (Panel B) Comparison of d(ATTA-GGCC-TAAT) (□) and d(ATTA-CGCC-TAAT) (●). Drug dissociation was initiated by adding an appropriate amount of 20% SDS solution to an ACTD (5μM) / DNA (40 μM) mixture. Kinetic traces were obtained via 453-nm monitoring in a 1-cm cell with use of a stirrer accessory.

Table 2: Comparison of Non-Stopped-Flow-Measurable ACTD Association and Dissociation Kinetics for Selected Dodecamers at 20 °C

oligomer	k_a (min^{-1})	k_d (min^{-1})
d(ATTA-TGCA-TAAT)	2.4	0.019
d(ATTA-AGCT-TAAT)	1.0	0.062
d(ATTA-CGCG-TAAT)	2.3	0.081
d(ATTA-GGCC-TAAT)		4.1
d(ATTA-AGCA-TAAT)	2.9	2.2
d(ATTA-TGCT-TAAT)[a]	1.3; 0.26 (48%)	0.20; 0.023 (68%)
d(ATTA-GGCG-TAAT)		1.9
d(ATTA-CGCC-TAAT)	4.8	2.2

[a] Values obtained via two-exponential fit, with the percent contribution only indicated for the slower component.

apparent (panel A) that the ACTD dissociation kinetic trace of the T/T-mismatched site is comparable to those of the self-complementary sequences but requires a two-exponential fit. Interestingly, its slower component ($k = 0.023$ min^{-1}) is only slightly faster than that of the -TGCA- site (0.019 min^{-1}) but is significantly slower than those of the -AGCT- (0.062 min^{-1}) and -CGCG- (0.081 min^{-1}) sequences (see Table 2). Furthermore, the ACTD dissociation rate from the GC site with flanking T/T mismatches is seen to be about 2 orders of magnitude slower than those of the other mismatches and that of -GGCC- (compare panels A and B; note the scale changes). It is also interesting to note that the association kinetics of ACTD to the dodecamer with T/T mismatches require a double-exponential fit. The slow component (0.26 min^{-1}) is significantly slower than the strong-binding self-complementary oligomers which can reasonably be approximated by single-exponential kinetics (1.0−2.4 min^{-1}) (see Table 2).

Effects of ACTD Binding on the Melting Temperatures of Oligomers. Thermal denaturation profiles with 275-nm monitoring for 40 μM DNA solutions in the absence and in the presence of ACTD were measured to investigate the effect of ACTD binding on the thermal stabilities of these oligomers. The results are included in Table 1. Due to the multiconformational states and the destabilization of the dimeric duplex resulting from the presence of base mismatches, these oligomers exhibit broad and diffuse melting profiles (not shown). The melting temperatures of the dimeric duplexes in 40 μM nucleotide solutions were estimated to be below 10 °C, from measurements with higher DNA concentrations. However, in the presence of 5 μM ACTD, the melting profile for the T/T-mismatched dodecamer exhibits a highly cooperative transition near 31 °C and the melting temperatures of the C/C and G/G mismatches have increased to about 23 and <20 °C, respectively. No apparent alteration on the melting profile was observed for the A/A-mismatched oligomer. These are to be compared with the melting temperatures of the strong-binding self-complementary dodecamers, which range from 34 to 43 °C, and the ACTD-induced melting temperature increases of 8−13 °C. The UV melting results of the DNA−ACTD complexes have also been corroborated by denaturation experiments via monitoring absorbance changes at 427 nm for the drug release (results not shown). Thus, the melting results also support the relative binding order established via spectral measurements.

Comparison with the Fluorescence Results of 7-Amino-actinomycin D. Although ACTD is only slightly fluorescent, its 7-amino derivative is strongly so. The amino group substitution does not greatly alter the intercalative binding mode of this derivative. It is, thus, of interest to corroborate the ACTD results with those of this derivative via fluorescence measurements. The fluorescence emission difference spectra with 560-nm excitation for the strong-binding self-complementary -XGCY-containing dodecamers exhibit a strong emission maximum near 650 nm (Figure 6A), suggesting fluorescence enhancements around this wavelength region when 7-AM-ACTD binds to these DNA. The much weaker binding of the -GGCC- sequence is again apparent via its negligible intensity enhancement. The fluorescence intensity induced by binding to the GC sequence with T/T mismatches (panel B) is seen to be comparable to that of the strong-binding self-complementary -XGCY- sequences. Interestingly, the intensity induced by binding to the site with flanking C/C mismatches is comparable to that of the self-complementary -CGCG- sequence. In contrast, the intensities for dodecamers with G/G mismatches are considerably smaller but are larger than those with A/A mismatches and -GGCC- sequence. The nearly identical spectral characteristics support the notion that the mode of binding at the GC site with flanking T/T mismatches is very similar to those of the strong-binding self-complementary -XGCY- sequences.

Kinetic measurements were also made by exciting the molecules with 560-nm light and monitoring emission at 650

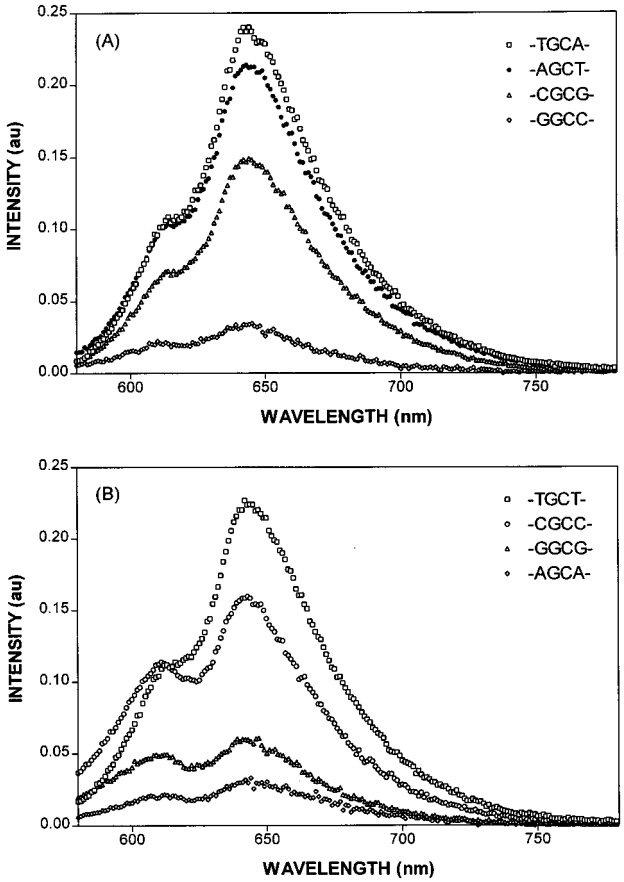

FIGURE 6: Comparison of fluorescence difference emission spectra (not corrected) at 20 °C of 1.5 μM 7-AM-ACTD in the presence of self-complementary dodecamers of the form d(ATTA-XGCY-TAAT) (panel A) and mismatched dodecamers of the form d(ATTA-XGCX-TAAT) (panel B). The spectra were obtained via 4-nm emission slit-width with 560-nm excitation and DNA concentrations of 40 μM.

Table 3: Comparison of 7-AM-ACTD Association and Dissociation Kinetics at 20 °C via Fluorescence Monitoring

oligomer	k_a (min^{-1})	k_d (min^{-1})
d(ATTA-TGCA-TAAT)	0.16	0.0031
d(ATTA-AGCT-TAAT)	0.12	0.011
d(ATTA-CGCG-TAAT)	0.22	0.014
d(ATTA-GGCC-TAAT)	5.8	1.5
d(ATTA-AGCA-TAAT)		6.0
d(ATTA-TGCT-TAAT)[a]	0.86; 0.16 (46%)	0.14; 0.022 (78%)
d(ATTA-GGCG-TAAT)		1.9
d(ATTA-CGCC-TAAT)	3.7	3.9

[a] Values obtained via two-exponential fit, with the percent contribution only indicated for the slower component.

nm for the association and at 600 nm for the SDS-induced dissociation of ACTD. Results of single- or double- (for the T/T-mismatched oligomer) exponential fits on these data are compared in Table 3. These results support our absorbance measurements indicating that the dodecamer with T/T mismatches flanking a GC sequence exhibits a much slower dissociation rate than those with C/C and other mismatches. It is worth noting that both the association and dissociation kinetics of 7-AM-ACTD in self-complementary oligomer solutions are considerably slower (some are almost an order of magnitude slower) than those of the parent ACTD but are not greatly different for the mismatched oligomers (compare Tables 2 and 3). This resulted in comparable association rates and much slower dissociation rates for

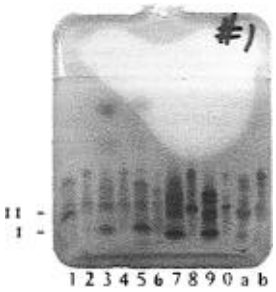

FIGURE 7: Comparison of electrophoretic mobility patterns of dodecamers at 4 °C in the absence (odd-numbered lanes and lane a) and in the presence (even-numbered lanes and lane b) of ACTD. Shown are d(ATTA-TGCA-TAAT) (lanes 1 and 2), d(ATTA-TGCT-TAAT) (lanes 3 and 4), d(ATTA-CGCC-TAAT) (lanes 5 and 6), d(AAAA-TGCT-TTTT) (lanes 7 and 8), d(AAAA-CGCC-TTTT) (lanes 9 and 0), and d(AAAA-TGCA-TTTT) (lanes a and b). [ACTD] = 0.17 mM and [DNA] was approximately 0.8 mM in nucleotides.

7-AM-ACTD at the -TGCA- sequence when compared to those at the T/T-mismatched site, contrary to the faster association rate and comparable dissociation rate observed for the parent ACTD.

Studies with d(AAAA-XGCX-TTTT). To see if the above results are peculiar to our chosen sequences of d(ATTA-XGCX-TAAT), studies were also made with dodecamers of the form d(AAAA-XGCX-TTTT) in which the terminal sequences have been altered. The results (not shown) confirm the strong binding and unusually slow dissociation of ACTD at the GC sequence with T/T flanking mismatches as well as weak binding at sequences with G/G and A/A mismatches. However, the observation of a significantly higher ACTD affinity and slower dissociation (still an order of magnitude faster than the T/T-mismatched oligomer) of d(AAAA-CGCC-TTTT) as compared to d(ATTA-CGCC-TAAT) manifests interesting sequence-dependent effects.

Electrophoretic Mobility Patterns of Oligomers and Their Drug Complexes. To further support the interpretation of our spectral results, electrophoretic measurements were made with dodecamers in the presence and in the absence of ACTD. Figure 7 compares the electrophoretic mobility patterns of selective oligomers at 4 °C. The multiconformational states of these oligomers are clearly evidenced by the presence of multiband and smearing features. The two self-complementary dodecamers d(ATTA-TGCA-TAAT) (lane 1) and d(AAAA-TGCA-TTTT) (lane a) are dominated by bands designated as II which can reasonably be assigned as those of dimeric duplex form. A slight retardation of this band is seen in the presence of ACTD (compare lanes 1 vs 2 and lanes a vs b), suggesting the formation of a complex with the dimeric duplex and the drug. Consistent with the dominant presence of hairpin species, all dodecamers with mismatches (lanes 3, 5, 7, and 9) exhibit prominent presence of electrophoretic bands designated as I which are considerably faster than those of the self-complementary counterparts. Despite the predominance of the hairpin form, the presence of ACTD resulted in the disappearance of band I and the appearance of retarded bands, which are nearly identical to those of the dimeric duplex−ACTD complexes of the self-complementary counterparts, for the T/T-mismatched oligomers (compare lanes 3 vs 4 and lanes 7 vs 8). Consistent with their weak ACTD binding affinities, oligomers containing G/G and A/A mismatches do not exhibit such retardations (results not shown). It is also interesting to note that whereas

d(ATTA-CGCC-TAAT) exhibits only intensity diminution of band I without the prominent appearance of the retarded dimeric duplex−ACTD complex band in the presence of ACTD (compare lanes 5 and 6), d(AAAA-CGCC-TTTT) induces retardation (compare lanes 9 and 0) that is very similar to that of T/T mismatches. This is consistent with the spectral results indicating that d(AAAA-CGCC-TTTT) exhibits stronger ACTD affinity than that of d(ATTA-CGCC-TAAT). These results support the notion of drug-induced allosteric conversion from hairpin to dimeric duplex and suggest that the binding affinities for the pyrimidine (pyr/pyr) mismatches are considerably higher than those with purine (pur/pur) mismatches.

It should be pointed out that possible impurities of 5% or less in our samples will not show up in our gel results. It is also interesting to note in passing that in addition to the prominent presence of the hairpin (I) and dimeric duplex (II) bands, a considerably slower moving band is apparent for each oligomer. The ACTD-induced retardation of its electrophoretic mobility is also clearly evident. It is reasonable to associate this band with that of the aforementioned tetrameric cruciform in which two of the side-arm duplexes contain GC sites. Indeed, the intensity of its retarded band is in concert with that of the corresponding ACTD-retarded band II of dimeric duplex, suggesting binding to the duplex side arms. It thus appears that despite the multiconformational states of the mismatched oligomers in solutions, our ACTD binding results largely reflect the relative ACTD binding affinities of -XGCX- in the duplex states.

DISCUSSION

Comparative electrophoretic, thermal denaturation, and spectroscopic studies with dodecamers of the form d(ATTA-XGCX-TAAT) and the corresponding self-complementary counterparts suggest that despite the dominance of hairpin conformations in solutions for mismatched oligomers, ACTD binds strongly to the GC sequence with flanking T/T mismatches and moderately to that with C/C mismatches but weakly to those of other homo-base mismatches. The relative binding order is found to be T/T > C/C > G/G > A/A. Spectral titrations indicate that the binding affinity of the T/T-mismatched dodecamer is comparable to or even stronger than the corresponding self-complementary -XGCY- sequences. However, the dodecamer with T/T mismatches exhibits surprisingly slow ACTD dissociation kinetics, with a rate more than an order of magnitude slower than those of oligomers with other mismatches but comparable to those of the -TGCA- and somewhat slower than the -AGCT- and -CGCG-containing sequences. The slow dissociation kinetic behaviors exhibited by this T/T-mismatched oligomer are corroborated by fluorescence measurements using 7-amino-ACTD, a fluorescent analog of ACTD. Fluorescence and absorbance spectral characteristics further indicate that the binding mode of the GC site with flanking T/T mismatches resembles those of the strong self-complementary -XGCY-containing sequences, which are known to be intercalative in nature.

The slow ACTD dissociation rate exhibited by the dodecamer containing T/T mismatches is rather unexpected, especially since it is comparable to that of the slow-dissociating -TGCA-containing dodecamer. One would have anticipated that the dimeric duplex destabilization caused by the presence of mismatched bases would have resulted in a very rapid drug dissociation. Thus, the observation of slow dissociation kinetics suggest that the T/T mismatches flanking the duplex 5′GC3′ site provide very favorable minor-groove environments (likely the consequence of its hydrophobicity and base size) for interactions with the pentapeptide rings of ACTD. In this connection, it may also be interesting to note that the site with C/C mismatches also exhibits significant ACTD affinity, whereas dodecamers with pur/pur mismatches exhibit unfavorable ACTD affinities. It thus appears that the bulkier purine bases result in a more distorted minor-groove environment, with the consequence of unfavorable interactions with the pentapeptide rings.

The unusual curvatures in the Scatchard plots exhibited by the mismatched dodecamers are also worth mentioning. This behavior may be understood by using the model presented in which the monomeric hairpin and dimeric duplex conformations are in dynamic equilibrium and ACTD only binds to the dimeric form. It can be shown that the Scatchard equation is now modified to $r/m = K_a (n - nL/L_t - r)$, where r, m, and n were defined in the legend of Figure 2 and L is the monomeric hairpin concentration. As L/L_t approaches unity (hairpin predominates), the equation reduces to a to a linear dependence of r/m vs r passing through the origin. On the other hand if L/L_t approaches zero (dimeric duplex predominates), the equation reduces to a regular Scatchard plot with the saturation binding density extrapolating to n. Thus, the exhibited unusual curvatures, with the appearance of data points emanating from the origin, can be seen as the consequence of the fact that the initial titration points correspond to dilute DNA concentrations, where monomeric hairpin conformations predominate, but later titration points eventually revert to "normal" Scatchard plots at higher DNA concentrations.

As noted earlier, the ACTD association kinetic trace for the dodecamer containing T/T mismatches requires a two-exponential fit with a significant contribution from a slow component which is considerably slower than those exhibited by the self-complementary sequences. The presence of this slow contribution and a multirate kinetic process may be the consequence of ACTD-induced allosteric conversion from the hairpin to the dimeric duplex form in drug binding.

The association as well as dissociation kinetics of 7-AM-ACTD are considerably slower than those of ACTD for the self-complementary sequences. This is consistent with the intercalative binding mode and the steric hindrance due to the presence of the amino group at the 7-position of ACTD. Such kinetic differentials between ACTD and 7-AM-ACTD are much less pronounced in the mismatched oligomers. This difference in kinetic behavior exhibited by the self-complementary vs mismatched sequences may likely be attributed to much lower duplex stabilities of the mismatched dimeric species and their drug complexes so that the hindrance presented by the 7-amino group becomes less critical.

Although the focus of this study is on the GC sequence with flanking homo-base mismatches, our results on the self-complementary dodecamers containing -XGCY- sequences are also of some interest. The dodecamer results are in general agreement with similar studies using decamers of the form d(ATA-XGCY-TAT) (Chen, 1988). The relative ACTD binding affinities are found to be -TGCA- > -CGCG- > -AGCT- >> -GGCC-, whereas the rate of ACTD

dissociation increases in the order -TGCA- < -AGCT- < -CGCG- << -GGCC-, with -TGCA- exhibiting the slowest dissociation kinetics. The fact that ACTD binds slightly more strongly to -CGCG- than to -AGCT- yet dissociates somewhat faster from the former suggests that the 2-amino group of guanine, which resides at the minor groove, may be one of the culprits of unfavorable interactions with the pentapeptide rings of the drug.

REFERENCES

Aivasashvilli, V. A,, & Beabealashvilli, R. S. (1983) *FEBS Lett. 160*, 124−128.

Akiyama, M., Maki, H., Sekiguchi, M., & Horiuchi, T. (1989) *Proc. Natl. Acad. Sci. U.S.A. 86*, 3949−3952.

Bailey, C., Graves, D. E., Ridge, G., & Waring, M. J. (1994) *Biochemistry 33*, 8736-8745.

Bailey, S. A., Graves, D. E., & Rill, R. (1994) *Biochemistry 33*, 11493−11500.

Bailey, S. A., Graves, D. E., Rill, R., & Marsch, G. (1993) *Biochemistry 32*, 5881−5887.

Brown, S. C., Mullis, K., Levenson, C., & Shafer, R. H. (1984) *Biochemistry 23*, 403−408.

Brown, D. R., Kurz, M., Kearns, D. R., & Hsu, V. L. (1994) *Biochemistry 33*, 651−664.

Chen, F.-M. (1988) *Biochemistry 27*, 6393−6397.

Chen, F.-M. (1992) *Biochemistry 31*, 6223−6228.

Chu, W., Shinomiya, M., Kamitori, K., Kamitori, S., Carlson, R. G., Weaver, R. F., & Takusagawa, F. (1994) *J. Am. Chem. Soc. 116*, 7971−7982.

Fasman, G. D., Ed. (1975) *CRC Handbook of Biochemistry and Molecular Biology*, 3rd ed., Vol. I, p 589, Chemical Rubber Company Press, Inc., Cleveland, OH.

Fletcher, M. C., & Fox, K. R. (1993) *Nucleic Acids Res. 21*, 1339−1344.

Fox, K. R., & Waring, M. J. (1984) *Nucleic Acids Res. 12*, 9271−9285.

Goodisman, J., & Dabrowiak, J. C. (1992) *Biochemistry 31*, 1058−1064.

Goodisman, J., Rehfuss, R., Ward, B., & Dabrowiak, J. C. (1992) *Biochemistry 31*, 1046−1058.

Hunter, W. (1992*) Methods in Enzymol. 211*, 221−231.

Kamitori, S., & Takusagawa, F. (1992) *J. Mol. Biol. 225*, 445−456.

Kamitori, S., & Takusagawa, F. (1994) *J. Am. Chem. Soc. 116*, 4154−4165.

Krugh, T. R. (1972) *Proc. Natl. Acad. Sci. U.S.A. 69*, 1911−1914.

Krugh, T. R., Mooberry, E. S., & Chiao, Y.-C. C. (1977) *Biochemistry 16*, 740−755.

Lane, M. J., Dabrowiak, J. C., & Vouurrnakis, J. N. (1983) *Proc. Natl. Acad. Sci. U.S.A. 80*, 3260−3264.

Liu, X., Chen, H., & Patel, D. J. (1991) *J. Biomol. NMR 1*, 323−347.

Modrich, P. (1987) *Annu. Rev. Biochem. 56*, 435−466.

Muller, W., & Crothers, D. M. (1968) *J. Mol. Biol. 35*, 251−290.

Patel, D. J. (1974) *Biochemistry 13*, 2396−2402.

Rehfuss, R., Goodisman, J., & Dabrowiak, J. C. (1990*) Biochemistry 29*, 777−781.

Rill, R. L., Marsch, G. A., & Graves, D. E. (1989) *J. Biomol. Struct. Dyn. 7*, 591−605.

Scamrov, A. V., & Beabealashvilli, R. Sh. (1983) *FEBS Lett. 164*, 97−101.

Scott, E. V., Jones, R. L., Banville, D. L., Zon, G., Marzilli, L. G., & Wilson, W. D. (1988) *Biochemistry 27*, 915−923.

Snyder, J. G., Hartman, N. G., D'Estantoit, B. L., Kennard, O., Remeta, D. P., & Breslauer, K. J. (1989) *Proc. Natl. Acad. Sci. U.S.A. 86*, 3968−3972.

Sobell, H. M., & Jain, S. C. (1972) *J. Mol. Biol. 68*, 21−34.

Takusagawa, F., Dabrow, M., Neidle, S., & Berman, H. M. (1982) *Nature 296*, 466-469.

Van Dyke, M. W., & Dervan, P. B. (1983) *Nucleic Acids Res. 11*, 5555−5567.

Van Dyke, M. W., Hertzberg, R. P., & Dervan, P. B. (1983) *Proc. Natl. Acad. Sci. U.S.A. 79*, 5470−5474.

Wadkins, R. M., & Jovin, T. M. (1991) *Biochemistry 30*, 9469−9478.

Waterloh, K., & Fox, K. R. (1992) *Biochim. Biophys. Acta 1131*, 300−306.

White, R. J., & Phillips, D. R. (1989) *Biochemistry 28*, 6259−6269.

Zhou, N., James, T. L., & Shafer, R. H. (1989) *Biochemistry 28*, 5231−5239.

BI961060D